ELSEVIER

Entropy generation rate during laser pulse heating: Effect of laser pulse parameters on entropy generation rate

H. Al-Qahtani, B.S. Yilbas*

KFUPM, Box 1913, Dhahran 31261, Saudi Arabia

Abstract

Laser pulse heating of solid surface and entropy generation during the heating process are considered. Time exponentially decaying pulse is accommodated in the analysis and the laser pulse parameter (β_1/β_2) resulting in minimum entropy generation rate is computed. Analytical solutions for temperature rise are presented and volumetric entropy generation rate is formulated. Two laser pulses resulting in low volumetric entropy generation rate are examined in detail and volumetric entropy generation rate is associated with the laser pulse parameter (β_1/β_2). It is found that volumetric entropy generation rate attains high values in the early heating period due to large ($1/T^2$). Moreover, the laser pulse with high-peak intensity results in lower volumetric entropy generation rate than that corresponding to the low-intensity laser pulse with the same energy content.
© 2007 Elsevier Ltd. All rights reserved.

Keywords: Laser; Pulse; Temperature; Entropy generation rate

1. Introduction

Laser pulse heating of solid surfaces finds application in metal industry due to rapid processing, precision of operation, and local treatment. In this case, the depth of annealed surface as shallow as a few μm to a fraction of μm can be achieved. Analytical modeling of the heating process provides closed form solution for temperature rise in the irradiated region. This, in turn, enables one to optimize the process parameters to reduce the experimental time and cost. The thermodynamic irreversibility in the thermal system lowers the second law efficiency and gives insight into the thermal quality of the process. Moreover, thermodynamic irreversibility can be quantified through entropy generation rate. Minimum entropy generation rate can be considered to be a key issue for the efficient thermal processing. Consequently, entropy generation rate can be minimized and laser pulse parameters resulting in minimum entropy generation rate can be identified for the efficient heating process. Therefore, investigation into entropy generation rate and identifying the laser pulse parameters minimizing entropy generation rate during the laser heating process becomes essential.

Considerable research studies were carried out to examine analytically the laser heating process. Ready [1] introduced analytical solution for a constant intensity laser pulse heating process. The closed form solution was limited with the constant intensity pulse applications. Yilbas [2] obtained a closed form solution for temperature rise during the laser heating process using the Laplace transformation method. His solution was also limited with the constant intensity pulse applications. Blackwell [3] provided analytical solution for the laser heating process. The closed form solution assumed exponentially decaying pulse and pulse variation including intensity change was neglected. Time exponentially varying pulse was considered by Yilbas [4] and the exact solution was obtained using the Laplace transformation method. However, the pulse optimization for efficient processing was left obscure in the study. Analytical model for laser pulse heating of embedded biological targets was presented by Mirkov et al. [5]. They developed a mathematical model for the laser-induced heating and cooling processes.

Laser pulse heating and entropy generation was investigated by Yilbas [6]. He formulated entropy generation

*Corresponding author. Tel.: +966 3 860 4481; fax: +966 3 860 2949.
E-mail address: bsyilbas@kfupm.edu.sa (B.S. Yilbas).

Nomenclature

C_P	specific heat (J/kg K)	T_2	temperature for first laser pulse parameter (β_2) (K)
I_0	laser peak power intensity (W/m^2)	$\dot{S}_{\text{gen}}$	volumetric entropy generation rate (W/m^{3}K)
k	thermal conductivity (W/m K)	$\dot{S}_{\text{gen}}^{*}$	dimensionless volumetric entropy generation rate
Q	heat flux (W/m^2)		
r_f	reflection coefficient	U	internal energy (J/kg)
t	time (s)	x	spatial location (m)
T	temperature (K)	α	thermal diffusivity (m^2/s)
T_1	temperature for first laser pulse parameter (β_1) (K)	β	laser pulse parameter (1/s)
		δ	absorption coefficient (1/m)
		ρ	density (kg/m^3)

rate and computed numerically during the heating and cooling phases of the laser pulse. Entropy generation rate during laser short-pulse heating was also examined by Yilbas [7]. He introduced entropy production rate due to thermal coupling of electron and lattice sub-systems. The irreversible thermodynamic analysis for thermal conduction was carried out by Jou and Casas-Vazquez [8]. They indicated that the irreversibility analysis provided useful information when the perturbation of the system were fast enough so that their frequency become comparable to the inverse of the relaxation times of the fluxes. However, in the analysis optimization of heating was not included.

In the present study, laser pulse heating of solid surface and entropy generation rate are considered. Time exponentially varying pulse is accommodated in the analysis to resemble the actual laser pulse and closed form solution for temperature rise is presented. Laser pulse parameter (β_1/β_2) resulting in minimum entropy generation rate is investigated.

2. Mathematical analysis

Mathematical analysis is composed of two parts, namely heating analysis and entropy analysis. Each analysis will be given under the appropriate subheadings.

2.1. Heating analysis

The schematic view of the laser heating process is shown in Fig. 1. Since the spot size is small (<1 mm) and the heat transfer in the radial direction is considerably smaller than its counterpart that takes place in the axial direction, one-dimensional heating model can be considered [9]. Laser heating pulse can be constructed from two time exponentially decaying pulses ($\exp(-\beta_1 t) - \exp(-\beta_2 t)$), where β_1 and β_2 are the laser exponential pulse parameters. The solution of conduction equation (the Fourier equation) can be obtained for only one exponential term ($\exp(-\beta_1 t)$) of the laser heating pulse; then, the solution for the second exponential term can be added to the solution of the first exponential term according to the superposition role. Consequently, temperature variation for the complete laser heating pulse can be obtained. In this case, the Fourier heat transfer equation due to time exponentially decaying laser pulse for the first term β

(β is used for the general purpose and it will be replaced with β_1 and β_2 later in the mathematical analysis) can be written as

$$\frac{\partial^2 T}{\partial x^2} + \frac{I_1 \delta}{k}(e^{-\beta t})e^{-\delta x} = \frac{1}{\alpha}\frac{\partial T}{\partial t}, \tag{1}$$

where

$$I_1 = (1 - r_f)I_0.$$

In the analysis, no heat convection is considered from the free surface of the substrate material. It should be noted that the convective heat loss from the surface is negligibly small during the laser heating pulse [10]. The depth well below the surface ($x \cong \infty$), temperature remains the same. Therefore, the corresponding boundary conditions are

at the surface:

$$\text{At } x = 0 \Rightarrow \left.\frac{\partial T}{\partial x}\right\|_{x=0} = 0.$$

at depth infinity:

$$\text{At } x = \infty \Rightarrow T(\infty, t) = 0.$$

Initially, substrate material is considered at uniform temperature. Hence, the initial condition is

Initially : At $t = 0 \Rightarrow T(x, 0) = 0.$

The Laplace Transformation of Eq. (1) with respect to t, results

$$\frac{\partial^2 \bar{T}}{\partial x^2} + \frac{I_1 \delta}{k}\frac{e^{-\delta x}}{(s + \beta)} = \frac{1}{\alpha}\left[s\bar{T}(x, s) - T(x, 0)\right]. \tag{2}$$

Laser Beam
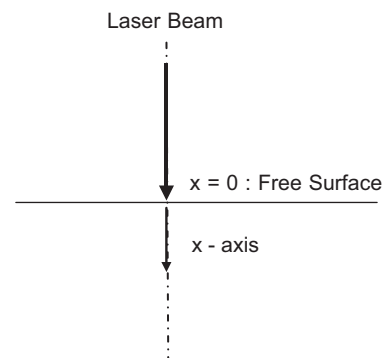
Fig. 1. Schematic view of laser heating and x-axis location.

Introducing the initial condition and rearranging Eq. (2) yields

$$\frac{\partial^2 \bar{T}}{\partial x^2} - h^2 \bar{T} = -\frac{I_1 \delta}{k} \frac{e^{-\delta x}}{(s+\beta)}, \tag{3}$$

where $h^2 = s/\alpha$ and s is the transform variable. Eq. (3) has the solution:

$$T(x,s) = Ae^{hx} + Be^{-hx} - \frac{I_1 \delta e^{-\delta x}}{k(s+\beta)(\delta^2 - h^2)}, \tag{4}$$

where A and B are constants. Introducing the boundary conditions will allow determining the constants A and B, i.e.

$$\bar{T}(x,s) = -\frac{I_1 \delta}{k(s+\beta)}\left[\frac{\delta \exp(-hx)}{h(h^2 - \delta^2)} - \frac{\exp(-\delta x)}{(h^2 - \delta^2)}\right], \tag{5}$$

which gives the solution for temperature in Laplace domain.

The inverse Laplace transform of Eq. (5) gives the temperature distribution inside the substrate material in space (x) and time (t) domain as follows [4]:

$$T(x,t) = \frac{I_1 \delta}{2k}\left(\frac{\alpha}{\beta + \alpha \delta^2}\right)\left\{ \begin{array}{l} i\delta\sqrt{\frac{\alpha}{\beta}}\exp(-\beta t)\left[\begin{array}{l} \exp\left(ix\sqrt{\frac{\beta}{\alpha}}\right)\text{Erfc}\left(\frac{x}{2\sqrt{\alpha t}} + i\sqrt{\beta t}\right) \\ -\exp\left(-ix\sqrt{\frac{\beta}{\alpha}}\right)\text{Erfc}\left(\frac{x}{2\sqrt{\alpha t}} - i\sqrt{\beta t}\right) \end{array}\right] \\ +\exp(\alpha\delta^2 t)\left[\begin{array}{l} \exp(\delta x)\text{Erfc}\left(\frac{x}{2\sqrt{\alpha t}} + \delta\sqrt{\alpha t}\right) - \exp(-\delta x)\text{Erfc}\left(\delta\sqrt{\alpha t} - \frac{x}{2\sqrt{\alpha t}}\right) \\ -2\exp(-(\beta t + \delta x)) \end{array}\right] \end{array}\right\}, \tag{6}$$

where Erfc is the complementary error function. Eq. (6) is the closed form solution for temperature distribution. The temperature distribution in non-dimensional form is possible by defining dimensionless quantities and substituting in Eq. (6).

The solution of complete laser heating pulse including both exponential terms is

For $\beta = \beta_1$,

Consequently, temperature variation for the complete laser heating pulse is

$$T(x,t)_{\text{complete pulse}} = T_1(x,t) - T_2(x,t). \tag{7}$$

The following dimensionless parameters are used for non-dimensionalized Equation (7):

$$x* = x\delta : t^* = \alpha\delta^2 t : \beta^* = \frac{\beta}{\alpha\delta^2} : T^* = \frac{T}{(I_1/k\delta)}.$$

Non-dimensional form of Eq. (7) is used to compute temperature distribution inside the substrate material for complete laser heating pulse.

2.2. Entropy analysis

Volumetric entropy generation rate in a thermal system can be written as [11]

$$\dot{S}_{\text{gen}} = \frac{1}{T}\nabla q - \frac{1}{T^2}q\nabla T + \rho\frac{DS}{DT}, \tag{8}$$

where

$$\rho\frac{DS}{DT} = \frac{\rho}{T}\frac{Du}{Dt} - \frac{P}{\rho T}\frac{D\rho}{Dt}.$$

Since the density remains constant for solids, the second term in Eq. (8) reduces to zero $((P/\rho T)(D\rho/Dt) = 0)$.

$$T_1(x,t) = \frac{I_1 \delta}{2k}\left(\frac{\alpha}{\beta_1 + \alpha \delta^2}\right)\left\{ \begin{array}{l} i\delta\sqrt{\frac{\alpha}{\beta}}\exp(-\beta_1 t)\left[\begin{array}{l} \exp\left(ix\sqrt{\frac{\beta_1}{\alpha}}\right)\text{Erfc}\left(\frac{x}{2\sqrt{\alpha t}} + i\sqrt{\beta_1 t}\right) \\ -\exp\left(-ix\sqrt{\frac{\beta_1}{\alpha}}\right)\text{Erfc}\left(\frac{x}{2\sqrt{\alpha t}} - i\sqrt{\beta_1 t}\right) \end{array}\right] \\ +\exp(\alpha\delta^2 t)\left[\begin{array}{c} \exp(\delta x)\text{Erfc}\left(\frac{x}{2\sqrt{\alpha t}} + \delta\sqrt{\alpha t}\right) - \exp(-\delta x)\text{Erfc}\left(\delta\sqrt{\alpha t} - \frac{x}{2\sqrt{\alpha t}}\right) \\ -2\exp(-(\beta_1 t + \delta x)) \end{array}\right] \end{array}\right\},$$

and for $\beta = \beta_2$:

$$T_2(x,t) = \frac{I_1 \delta}{2k}\left(\frac{\alpha}{\beta_2 + \alpha \delta^2}\right)\left\{ \begin{array}{l} i\delta\sqrt{\frac{\alpha}{\beta}}\exp(-\beta_2 t)\left[\begin{array}{l} \exp\left(ix\sqrt{\frac{\beta_2}{\alpha}}\right)\text{Erfc}\left(\frac{x}{2\sqrt{\alpha t}} + i\sqrt{\beta_2 t}\right) \\ -\exp\left(-ix\sqrt{\frac{\beta_2}{\alpha}}\right)\text{Erfc}\left(\frac{x}{2\sqrt{\alpha t}} - i\sqrt{\beta_2 t}\right) \end{array}\right] \\ +\exp(\alpha\delta^2 t)\left[\begin{array}{c} \exp(\delta x)\text{Erfc}\left(\frac{x}{2\sqrt{\alpha t}} + \delta\sqrt{\alpha t}\right) - \exp(-\delta x)\text{Erfc}\left(\delta\sqrt{\alpha t} - \frac{x}{2\sqrt{\alpha t}}\right) \\ -2\exp(-(\beta_2 t + \delta x)) \end{array}\right] \end{array}\right\}.$$

Therefore, Eq. (8) becomes

$$\dot{S}_{\text{gen}} = \frac{1}{T} \nabla q - \frac{1}{T^2} q \nabla T + \frac{\rho}{T} \frac{Du}{Dt}. \tag{9}$$

The term $(\rho/T)(Du/Dt)$ in one-dimensional solid can be written as

$$\frac{\rho}{T} \frac{Du}{Dt} = \frac{1}{T}(-\nabla q). \tag{10}$$

Combining Eqs. (9) and (10) results in

$$\dot{S}_{\text{gen}} = \frac{1}{T} \nabla q - \frac{1}{T^2} q \nabla T - \frac{1}{T}(\nabla q). \tag{11}$$

However, $q = -k\nabla T$. Consequently, re-arrangement of Eq. (11) yields

$$\dot{S}_{\text{gen}} = \frac{k}{T^2}(\nabla T)^2. \tag{12}$$

Non-dimensional form of Eq. (12) can be written as

$$\dot{S}_{\text{gen}}^* = \frac{1}{T^{*2}}(\nabla T^*)^2, \tag{13}$$

where $\dot{S}_{\text{gen}}^* = \dot{S}_{\text{gen}}^*(1/k\delta)$.

Eq. (13) is used to compute dimensionless entropy generation rate.

3. Results and discussions

Laser pulse heating and entropy generation rate for pulse optimization are considered. The closed form solution for temperature rise due to time exponentially varying pulse is used to obtain temperature and entropy change in the substrate material. The pulse parameter (β_1/β_2) resulting in minimum entropy generation rate is obtained.

Fig. 2 shows a three-dimensional view of volumetric entropy generation rate for three different time and space domains. The x- and y-axes of the figure represent the laser pulse parameters β_1 and β_2. In all time and space domains considered in the present analysis, volumetric entropy generation rate behaves in such a way that increasing both β_1 and β_2 results in low entropy generation rate. Consequently, for laser pulses resulting in low entropy generation rate must have relatively large values of β_1 and β_2 pulse parameters. This is mainly because of attainment of relatively high temperature and low temperature gradients for large values of β_1 and β_2 (Eq. (7)). Consequently, two values of pulse parameters β_1 and β_2 are selected in accordance with low entropy generation rate for further examinations.

Fig. 3 shows two laser pulses used in the simulations. It should be noted that the pulse energy for both pulses remains the same. Two pulses with different parameters can be distinguished for their peak pulse intensities, i.e. one pulse has higher peak intensity than the other, despite the fact that both pulses have the same energy content. Fig. 4 shows temporal variation of temperature for two pulses with different pulse parameters. Temperature rise is high in the early heating period and the maximum surface
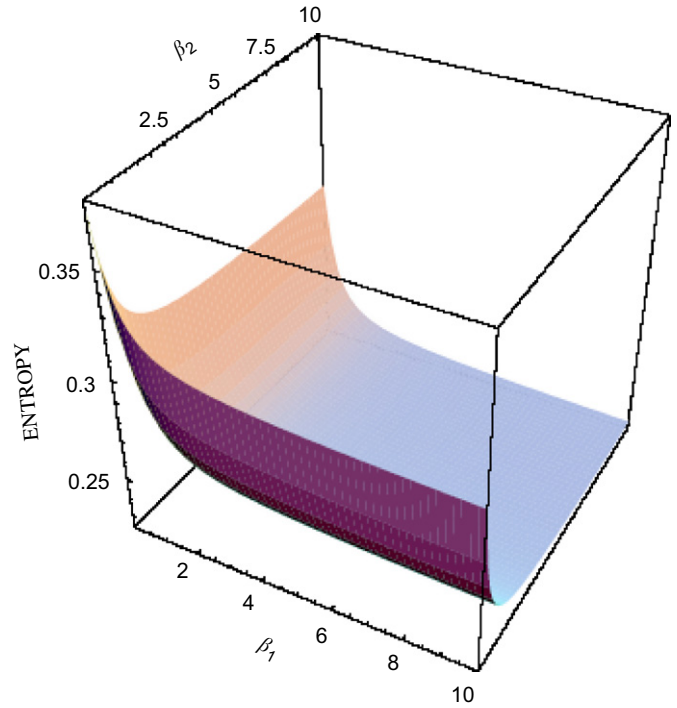
Fig. 2. Three-dimensional view of volumetric entropy generation rate with pulse parameters β_1 and β_2.
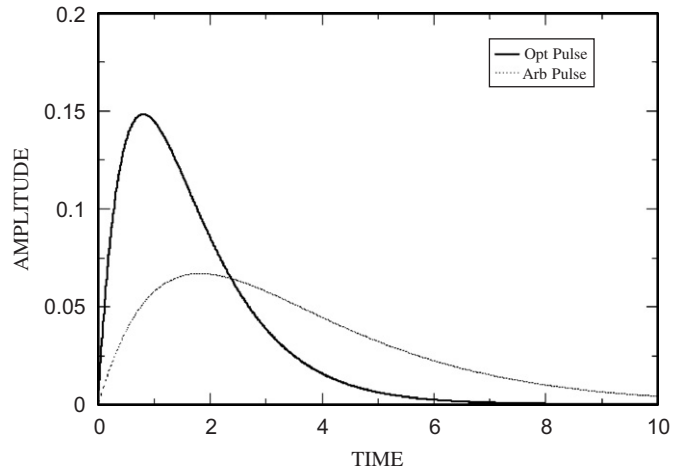
Fig. 3. Time exponentially varying pulses used in the simulations. Opt. pulse has the high-peak intensity while Arb. pulse is the low-peak intensity, provided that pulse energy for both pulses remains the same.

temperature occurs when the pulse intensity reaches its maximum. However, temperature rise does not exactly follow the laser pulse profile, which is due to diffusion and energy transport from the surface region to the solid bulk. This, in turn, lowers the temperature in the surface region. The decay rate of temperature profiles corresponding to both pulses are similar despite the fact that decay rate of both pulses are notably different. This indicates that once the temperature field is developed after reaching the maximum temperature at the surface, diffusional energy transfer from the surface region to the solid bulk becomes
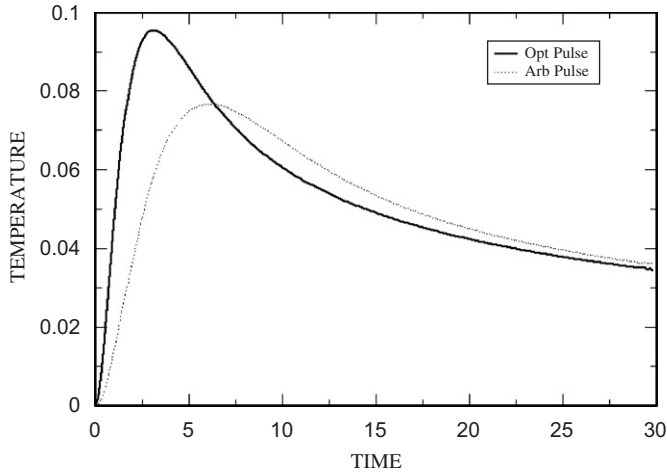
Fig. 4. Temporal variation of dimensionless temperature for two pulses employed in the simulations.
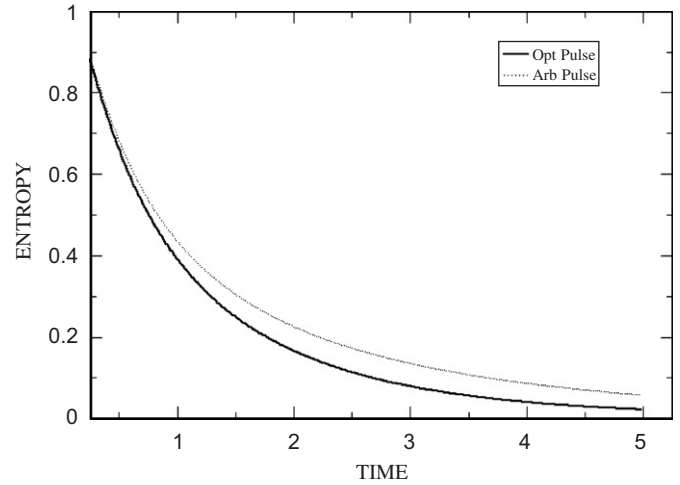
Fig. 6. Temporal variation of dimensionless entropy generation rate for two pulses employed in the simulations.
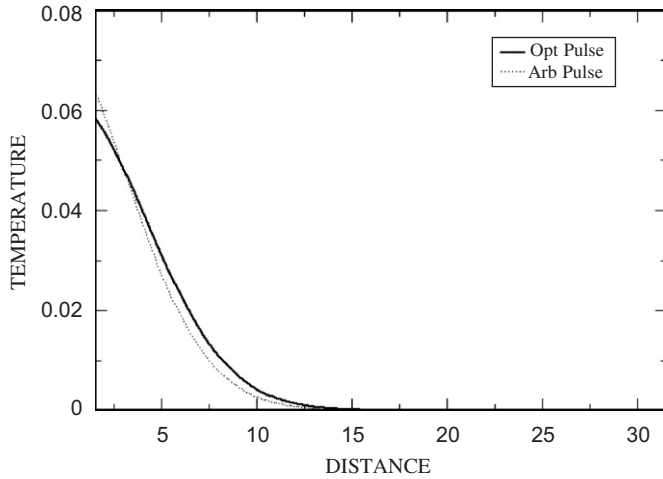
Fig. 5. Dimensionless temperature distribution inside the substrate material for two pulses employed in the simulations.
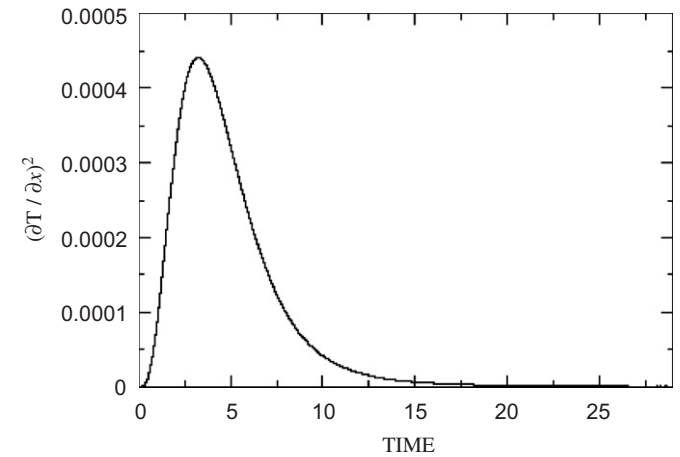
Fig. 7. Temporal variation of dimensionless temperature square at a depth of $x = 1$ for two pulses employed in the simulations.

high for high-peak intensity pulse due to high-temperature gradient developed in the surface region. It should be noted that high-temperature gradient accelerates the diffusional energy transport from the surface region to the solid bulk.

Fig. 5 shows temperature distribution inside the substrate material for two pulses with different pulse parameters. Temperature decays sharply with increasing depth below the surface for both pulses, provided that temperature gradient is high for the high-peak intensity pulse. This, in turn, increases conduction from the surface region to the solid bulk. In addition, absorption inside the substrate material is governed by the Lambert's law, in which case, absorbed laser intensity decays exponentially inside the substrate material. The decay of temperature in the surface vicinity is smaller than that corresponding to the region next to the surface vicinity. This is because of energy gain from the irradiated field, which is high in the surface vicinity, and low temperature gradient in this region, which lowers the conduction loss from the surface

vicinity. However, as the depth below the surface increases in the region next to surface vicinity, energy gain from the irradiated field reduces, which in turn results in attainment of low temperature in this region. This causes increase in temperature gradient in the region between the surface vicinity and next to the surface vicinity. Consequently, temperature gradient becomes high and conduction losses from the surface vicinity increases.

Fig. 6 shows temporal variation of entropy generation at the surface for two laser pulses with different pulse parameters. Both pulses result in similar entropy generation rate in the early heating period due to low $(dT/dx)^2$, which can also be observed from Fig. 7. As the heating period progresses volumetric entropy generation rate differs for both pulses and high-peak intensity pulse gives rise to less entropy generation rate. This is because of the attainment of high temperature and low $1/T^2$ (as seen from Fig. 8). However, as the heating period progresses further, the difference in volumetric entropy generation rate due
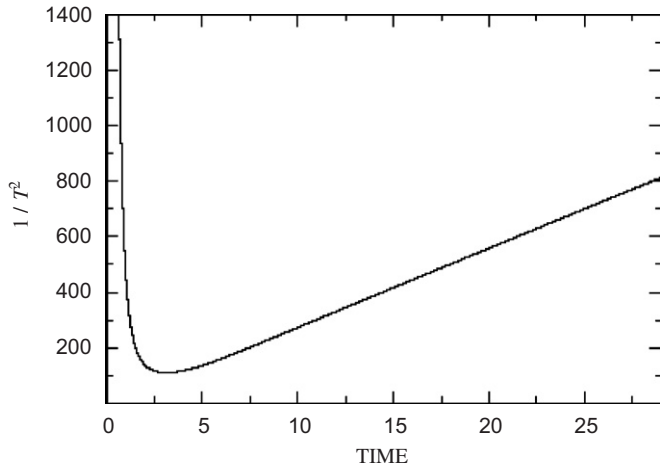
Fig. 8. Temporal variation of $1/T^2$ at a depth of $x = 1$ for two pulses employed in the simulations.
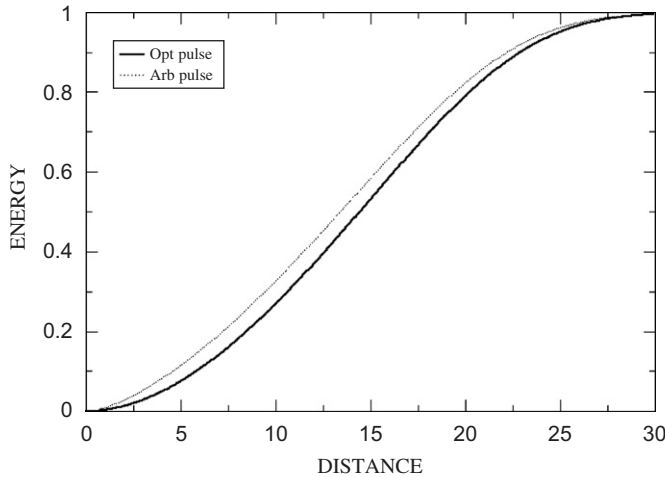
Fig. 9. Dimensionless entropy generation rate inside the substrate material at $t = 10$ for two pulses employed in the simulations.

to both pulses becomes large despite the fact that both $(dT/dx)^2$ and $(1/T^2)$ become small for both pulses. This is because of the difference in temperatures and the gradients due to both pulses. In this case, temperature remains high while temperature gradient is low for the high-intensity pulse. Consequently, volumetric entropy generation rate becomes lower for the high-peak intensity pulse than for the corresponding other pulse.

Fig. 9 shows volumetric entropy generation rate inside the substrate material for two pulses with different pulse parameters. Volumetric entropy generation rate is low in the surface region due to low $1/T^2$ and (dT/dx). However, as the distance increases away from the surface towards the solid bulk, entropy generation rate increases because of reducing temperature and increasing temperature gradient in this region. As the depth below the surface increases further, temperature gradient and temperature reduce significantly. Moreover, entropy generation rate increases further with increasing depth despite the attainment of the low-tempera-

ture gradient. The increase in entropy generation rate is associated with temperature reduction with increasing depth, i.e., $1/T^2$ increases significantly with increasing depth below the surface. Consequently, increase in $1/T^2$ suppresses the decay in (dT/dx) and results in high rate of volumetric entropy generation at depth further away from the surface. The difference in both entropy profiles due to two pulses is evident. However, this difference ceases once the depth below the surface increases further towards the solid bulk where temperature becomes almost the same for both pulses.

4. Conclusion

Laser pulse heating is considered and volumetric entropy generation rate is formulated. Time exponentially varying pulse profiles are considered and the laser pulse parameter (β) resulting in the minimum entropy generation rate in the solution domain is determined. In this case, entropy field is computed for various values of the laser pulse parameters and two values of pulse parameters are selected for further analysis. Temperature and entropy fields are predicted for two time exponentially decaying pulse with different pulse parameters. The energy content in both pulses is kept the same. It is found that temporal variation of temperature at the surface does not follow the laser pulse variation because of the diffusional energy loss from the surface region to the solid bulk. Surface temperature rises rapidly for the pulse with high peak intensity. This results in rapid decay of temperature in the cooling period. Temperature gradient is low in the surface region due to internal energy gain from the irradiated field and it increases sharply as the depth below the surface increases towards the solid bulk. The exponential pulse with high-peak intensity results in high-temperature gradient in the region next to the surface vicinity. Volumetric entropy generation rate attains low values in the surface region and as the distance from the surface increases it increases despite the fact that temperature gradient reduces. In this case, $1/T^2$ amplifies volumetric entropy generation rate. Volumetric entropy generation rate attains high values in the early heating period because of attainment of low temperature in this period. Volumetric entropy generation rate due to both pulses differs in the surface region as the heating period progresses. This is because of the differences in temperature, i.e., $1/T^2$ differs for both pulses. The laser with high peak intensity results in low-entropy generation rate, which in turn indicates the possible attainment of efficient heating process.

Acknowledgements

References

[1] Ready JF. Effects due to absorption of laser radiation. J Appl Phys 1963;36:462–70.

[2] Yilbas BS. Analytical solution for heat conduction mechanism appropriate to the laser heating process. Int Commun Heat Mass Trans 1993;20:545–55.

[3] Blackwell FJ. Temperature profile in semi-infinite body with exponential source and convective boundary conditions. ASME J Heat Trans 1990;112:567–71.

[4] Yilbas BS. Analytical solution for time unsteady laser pulse heating of semi-infinite solid. Int J Mech Sci 1997;39(6):671–82.

[5] Mirkov M, Sherr EA, Sierra RA, Lloyd JR, Tanghetti E. Analytical modeling of laser pulse heating of embedded biological targets: an application to cutaneous vascular lesions. J Appl Phys 2006;99: 114701.

[6] Yilbas BS. Three-dimensional laser heating model and entropy generation consideration. ASME J Energy Resource Technol 1999;121:217–24.

[7] Yilbas BS. Entropy production during laser picosecond heating of copper. ASME J Energy Resource Technol 2002;124:204–13.

[8] Jou D, Casas-Vazquez J. Extended irreversible thermodynamics of heat conduction. Eur J Phys 1988;9:329–33.

[9] Yilbas BS, Sami M. Three-dimensional laser heating including evaporation—a kinetic theory approach. Int J Heat Mass Trans 1998;41(13):1969–81.

[10] Shuja SZ, Yilbas BS. 3-dimensional conjugate heating of a moving slab. Appl Surf Sci 2000;167:134–48.

[11] Bejan A. Entropy generation minimization. New York: CRC press; 1995.